2-2007

Fluctuations and patterns in nanoscale surface reaction systems: Influence of reactant phase separation during CO oxidation

Da-Jiang Liu
Ames Laboratory, dajiang@fi.ameslab.gov

James W. Evans
Iowa State University, evans@ameslab.gov

Fluctuations and patterns in nanoscale surface reaction systems: Influence of reactant phase separation during CO oxidation

Abstract
A realistic atomistic model is used to assess spatiotemporal behavior in nanoscale CO oxidation systems at higher pressures than for traditional ultrahigh vacuum studies. The strong influence of adspecies interactions in this regime of high reactant coverages leads to phase separation between oxygen-rich and CO-rich reactive states. Time-series studies reveal fluctuation-induced transitions between these states, as well as transitions between reactive and inactive states. In addition, we observe flickering spatial patterns with sharp boundaries.

Disciplines
Mathematics | Physical Chemistry

Comments
This article is from *Physical Review B* 75 (2007): 073401, doi: 10.1103/PhysRevB.75.073401. Posted with permission.

Fluctuations and patterns in nanoscale surface reaction systems: Influence of reactant phase separation during CO oxidation

Da-Jiang Liu[1] and J. W. Evans[1,2]
[1]*Ames Laboratory–USDOE, Iowa State University, Ames, Iowa 50011, USA*
[2]*Department of Mathematics, Iowa State University, Ames, Iowa 50011, USA*
(Received 30 November 2006; published 2 February 2007)

A realistic atomistic model is used to assess spatiotemporal behavior in nanoscale CO oxidation systems at higher pressures than for traditional ultrahigh vacuum studies. The strong influence of adspecies interactions in this regime of high reactant coverages leads to phase separation between oxygen-rich and CO-rich reactive states. Time-series studies reveal fluctuation-induced transitions between these states, as well as transitions between reactive and inactive states. In addition, we observe flickering spatial patterns with sharp boundaries.

DOI: 10.1103/PhysRevB.75.073401 PACS number(s): 82.40.Np, 68.43.Jk, 82.65.+r

Catalytic reactions have been studied extensively by the surface science community mainly on extended single-crystal surfaces. However, recent interest has turned to analysis of reactions in nanoscale systems, e.g., on supported metal clusters[1] or on metal field emitter tips (FET's) with facet linear dimensions of $\sim$10 nm.[2] In these systems, fluctuation effects occur specifically due to their small size. For example, CO oxidation on extended surfaces typically exhibits robust bistability. Stable reactive and near-CO-poisoned inactive states coexist in some region of the (P,T)-plane, where P denotes a suitable partial pressure and T denotes surface temperature. This bistability derives from the nonlinear Langmuir-Hinshelwood kinetics together with long-range spatial coupling due to facile CO surface diffusion.[3,4] However, experimental studies for nanoscale systems suggest a loss of bistability due to noise-induced transitions between stable branches.[1,2] One might also anticipate the occurrence of nonequilibrium critical phenomena near the cusp point which terminates the bistable region.[3,5]

At lower P or higher T, the high mobility, low coverages, and weak effective interactions for reactant adspecies imply that mean-field-type dynamics is operative. Nanoscale fluctuation behavior in this regime has been analyzed by (i) mean-field birth-death-type master equations and corresponding stochastic Gillespie-type simulations for the evolution of numbers of reactant adspecies; and (ii) kinetic Monte Carlo (KMC) simulation of hybrid models with a mean-field treatment of infinitely mobile CO and a lattice-gas treatment of oxygen incorporating minimal adspecies interactions.[2,5–8] Such analyses reveal that the rate of transitions between stable branches decreases exponentially with system size (surface area). These analyses also quantify the enhancement of transitions near the cusp point.[6]

However, field-ion or field-emission microscopy studies of fluctuations in reactions on metal FET's are often performed at lower T down to 300 K.[2,9–11] In reaction studies on supported nanoclusters where fluctuation effects are also important,[1] the ultimate goal is to elucidate behavior at higher P closer to industrial conditions.[12] In such regimes of higher P or lower T, the effect of adspecies interactions within the higher-coverage reactant adlayers will generally produce additional strongly non-mean-field phenomena which can only be described by more complex and realistic atomistic modeling. The example on which we focus here is the occurrence and experimental ramification of equilibrium-type phase transitions corresponding to phase separation of reactants into oxygen-rich and intermixed reactive states.

In this paper, we use a realistic atomistic multisite lattice-gas model to explore CO oxidation in nanoscale systems at higher P or lower T. KMC simulations of the model reveal the existence of reactant phase separation, and are used to assess its influence on both fluctuation behavior and spatial pattern formation. First, time series for coverages are shown to display well-defined fluctuation-induced transitions between two phase-separated reactive states. These transitions, which appear similar to those observed in studies on metal FET's, have distinct characters from transitions in mean-field-type models. Second, strong adspecies interactions produce fluctuating spatial patterns which are sharp on the atomic scale. This contrasts reaction-diffusion patterns on extended surfaces under typical low-pressure conditions which are smeared on the scale of microns.[3]

The atomistic lattice-gas model utilized in this study has been constructed to provide a realistic description of CO oxidation on unreconstructed metal(100) substrates.[13] In addition to an appropriate description of CO adsorption-desorption kinetics, and dissociative adsorption kinetics for O_2, the selected adspecies interactions are chosen to recover observed adlayer ordering. However, just as significant for the current study is the feature that adsorbates can reside on different types of sites. This latter feature together with the inclusion of appropriate short-range exclusion or repulsion between CO and O facilitates reactant phase separation at sufficiently high adspecies coverages. Parameters in our modeling are chosen for CO+O/Pd(100):[13] O sits on hollow sites; CO sits on bridge sites at lower coverage and hollow sites at higher coverages (especially under reaction conditions); the model recovers the observed $c(2\sqrt{2}\times\sqrt{2})R45°$-CO ordering, and $p(2\times2)$-O and $c(2\times2)$-O ordering, as well as temperature-programmed desorption spectra; reaction configurations and activation barriers were based on density functional theory predictions. However, we remark that the basic feature of the model of interest here, specifically reactant phase separation, should be somewhat generic.

In presenting results below, for convenience we define effective partial pressures $\tilde{P}$ for CO and O_2 as the impingement rate times the low-coverage sticking coefficient of CO

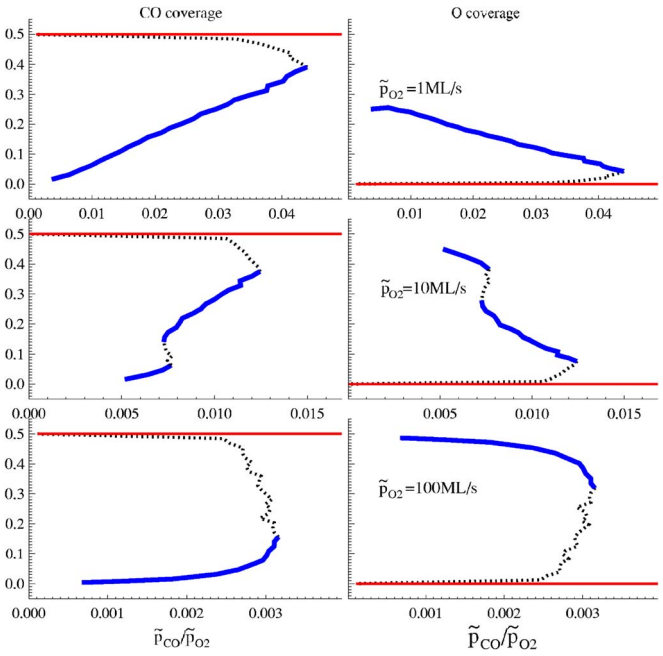

FIG. 1. (Color online) Steady state coverage of CO and oxygen for CO oxidation on Pd(100) at $T=350$ K. Blue lines represent stable reactive states, and red lines represent the stable CO-poisoned state. Dotted lines represent the unstable state.

and O_2 on a clean surface. Figure 1 shows the dependence on the ratio of effective partial pressures of the steady-state coverages for the reaction at 350 K for a "perfect" 32×32 site system with periodic boundary conditions. Results were obtained from constant CO-coverage simulations[14] which can access both stable and unstable steady states. For low $\tilde{P}_{O_2}=1$ ML/s, the coverage displays the traditional S shape for a bistable system with a stable inactive state (with high CO coverage $\theta_{CO}\approx0.5$ ML) and a stable reactive state (with lower θ_{CO}). However, increasing $\tilde{P}_{O_2}$ to 10 ML/s, a discontinuous jump develops in the reactive branch of the steady-state coverages. This is indicative of equilibrium-like phase separation between two reactive states. The first is a $c(2\times2)$-O ordered state with low θ_{CO} and high θ_O, and the second is a disordered state with moderate θ_{CO} and θ_O. See Fig. 2. Further increasing $\tilde{P}_{CO}$ to 100 ML/s, this discontinuity expands towards the inactive state, and the second reactive phase becomes unstable.

As an aside, we note that our simulations were performed with CO hop rates below physical values to enhance computational efficiency. These hop rates must be far above other rates to correctly describe local adlayer equilibration. We typically use $h_{CO}=10^3-10^4$ s^{-1} for hopping of isolated CO.

Studies on FET's have the major advantage over other techniques in that one can monitor *in situ* in real-time fluctuations in quantities related to reactant coverages. Thus, we next present in Fig. 2 simulated time series for the CO coverage at 350 K with $\tilde{P}_{O_2}=10$ ML/s (noting that similar behavior is exhibited by the O coverage and other quantities). We choose $\tilde{P}_{CO}/\tilde{P}_O=0.076$ corresponding to the value for phase separation. Then, well-defined transitions caused by internal fluctuations can be observed between the two reactive phases. The resulting CO-coverage distribution has a bimodal distribution where the two peaks have roughly equal weight. As $\tilde{P}_{CO}/\tilde{P}_O$ deviates slightly from this value, the distribution quickly becomes very skewed towards the true stable reactive state (the other being at best metastable).

One should also expect this model to produce distinct spontaneous transitions between the reactive and near-CO-poisoned phases. This should result in an associated bimodal coverage distribution with roughly equal weighted peaks near the appropriate equistability pressure ($\tilde{P}_{CO}/\tilde{P}_{CO}\approx0.011$ for $\tilde{P}_{O_2}=10$ ML/s at $T=350$ K). However, at $T=350$ K, CO desorption is strongly inhibited and the near-CO-poisoned phase with almost perfect $c(2\sqrt{2}\times\sqrt{2})R45°$ ordering is practically an absorbing state implying a very long residence time between transitions. To observe these transitions in a reasonable time frame, one can either introduce

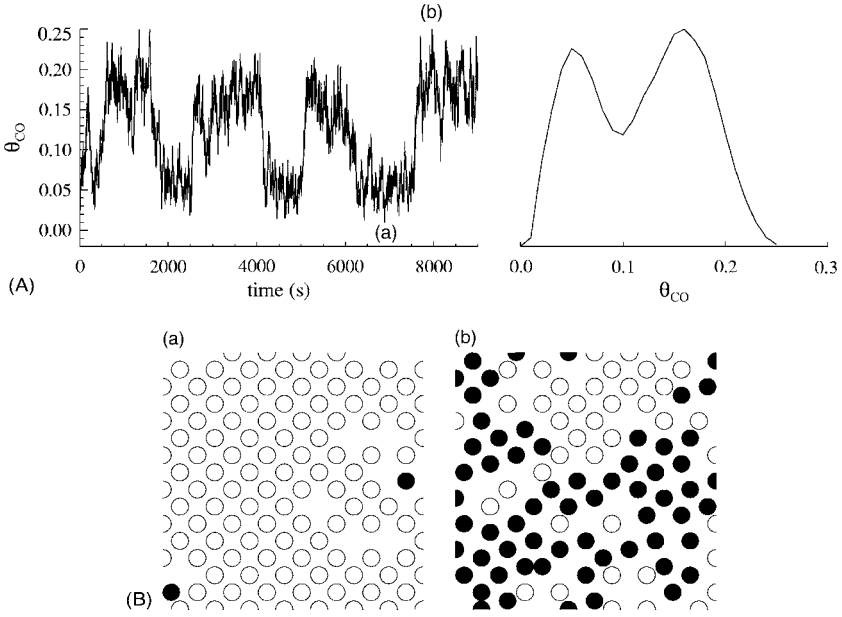

FIG. 2. Top left: fluctuations in CO coverage for CO oxidation in a 16×16 site system at $T=350$ K with $\tilde{P}_{O_2}=10$ ML/s and $\tilde{P}_{CO}=0.076$ ML/s. Top right: the corresponding CO coverage distribution. Bottom: state of the adlayer at different times (indicated) corresponding to oxygen-rich and CO-rich reactive states. CO: closed circles, oxygen: open circle.

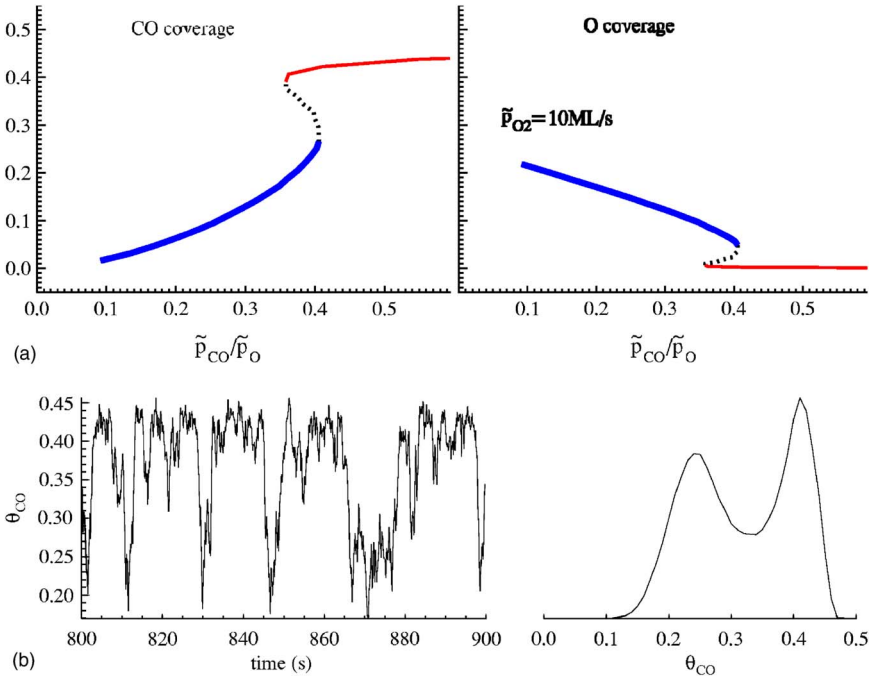

FIG. 3. (Color online) Top: steady-state coverage of CO and oxygen for CO oxidation at $T=440$ K with $\tilde{P}_{O_2}=10$ ML/s. Bottom: fluctuations in CO coverage for CO oxidation in a 16×16 site system under the above conditions with $\tilde{P}_{CO}=3.7$ ML/s.

"defects" or reduce the system size or increase the temperature closer to the cusp point. Figure 3 shows the steady-state coverage versus partial pressure for higher $T=440$ K with $\tilde{P}_{O_2}=10$ ML. Also shown are transitions in the CO coverage between the reactive and inactive states as well as the corresponding coverage bimodal distribution choosing $\tilde{P}_{CO}/\tilde{P}_{CO}$ close to the shifted equistability point.

Next, we provide a more detailed picture of the transitions discussed above. In a mean-field analysis of transitions in a perfect (defect free) bistable reaction system, transitions occur "homogeneously" as a result of coverage fluctuations. The mean-field kinetics produces an effective potential barrier per unit area, δV_{eff}, to transitions which vanishes approaching the bistability cusp. The rate of transitions is given by $k\sim\exp(-E_{\text{eff}})$, with $E_{\text{eff}}=L^2\delta V_{\text{eff}}$, and thus decreases strongly with system size.[6] This picture applies for transitions between reactive and inactive states. In contrast, transitions associated with reactant phase separation are not homogeneous. Patches of the O-rich reactive phase can nucleate within the intermixed reactive phase separated by a sharp phase boundary (and visa versa). In an extended system, these droplets would eventually shrink and disappear due to the effects of interface tension. However, in a nanoscale system they are likely to grow (randomly) and take over the entire system corresponding to an observed transition. In this scenario, one has $E_{\text{eff}}\sim L$ scaling with phase boundary length, so the transition rate does not decrease as quickly with increasing system size, a feature consistent with our simulated time series.

Some important aspects of experimental studies on FET's not addressed above are considered below. Often hysteresis analyses are performed in FET or conventional surface reaction studies where either temperature or a suitable partial pressure is swept back and forth across the bistable region. The resulting hysteresis loop is used to map out the boundaries of the bistable region, an approach which assumes both robust bistability and facile relaxation to stable states (on the time scale of sweeping). Figure 4 shows CO-coverage behavior at $T=350$ K obtained by sweeping $\tilde{P}_{CO}$ (starting from 0) for fixed $\tilde{P}_{O_2}=10$ ML/s. If one lets θ_{CO} increase to only 0.35 ML so that the system is far from CO poisoned, one obtains a hysteresis loop associated with reactant phase separation whose width reflects slow relaxation on the time scale of sweeping. The lower branch (pluses) is characterized by long range $c(2\times2)$-O layers, mixed with small amount of CO. The upper branch (a: diamonds) is characterized by intermingled CO and O patches with local ordering. In contrast, if one lets θ_{CO} increase near its inactive state value of 0.5 ML, then the upper branch (c: crosses) corresponds to near-perfect $c(2\sqrt{2}\times\sqrt{2})R45°$-CO ordering and persists to near $\tilde{P}_{CO}=0$. The hysteresis loop then does reflect reaction

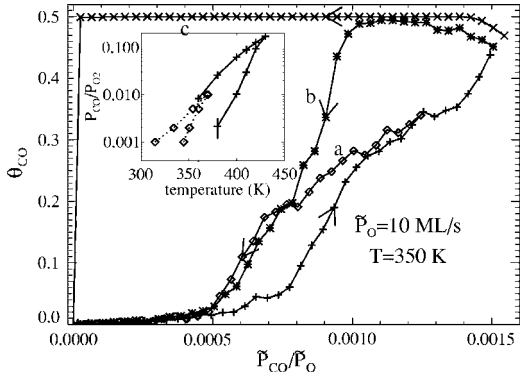

FIG. 4. Hysteresis analysis at 350 K with $\tilde{P}_{O_2}=10$ ML/s for a 32×32 site system with each data point averaged over 40 s. The three branches for the reverse sweep start from the stable reactive phase (a); the CO-poisoned phase with (b) and without (c) domain boundaries. Inset, bifurcation diagrams obtained from sweeps of type (c) corresponding to typical "reaction bistability" (solid lines), and of type (a) reflecting phase separation of the reactive state (dotted lines).

bistability, and repeating this scan for different conditions allows one to map the bistability region (inset of Fig. 4).

If during the hysteresis sweep, the system is unable to reach the near perfect $c(2\sqrt{2}\times\sqrt{2})R45°$-CO ordered inactive state (either due to some persistent domain boundary, or due to model modification to include "defect sites" inhibiting such ordering), then a narrower hysteresis loop results. Behavior for a domain boundary [(b) asterisks] is also shown in Fig. 4. Indeed, more generally, we find that introduction of various types of defects significantly shrinks the bistability region, consistent with experimental observations.[1]

Finally, we comment on two specific aspects of the experimental time-series studies of fluctuation-induced transitions and associated bimodal distributions. First, these studies can be coupled with a hysteresis analysis to conveniently identify regions of parameter space where a bimodal distributions will be observed (i.e., the middle of the hysteresis loop).[2] Without the hysteresis data, it is difficult to determine the (P,T) parameters producing such distributions. Second, in experimental studies, the time-series data often correspond not to coverage behavior on an entire nanofacet, but rather on a subwindow of such a facet. This introduces additional nuances to time-series interpretation. To illustrate these issues, we perform additional hysteresis simulations on a 32×32 site system with $T=350$ K and $\tilde{P}_{O_2}=10$ ML/s and extract real-space configurations for the entire system and time series for the CO coverage in a 16×16 site subwindow over a time interval which includes sweeping across the equilibrium phase transition ($\tilde{P}_{CO}/\tilde{P}_{O}$ decreasing from 0.007 to 0.005). The time-series displays large transitionlike fluctuations, but their characterization is rather distinct from above.

From Fig. 5, one can see that the system is characterized by interconnected CO and oxygen rich patches roughly corresponding to the two coexisting reactive states. During the time shown in Fig. 5, patches "flicker" in and out of existence from the subwindow, leading to strong fluctuations in CO coverage. The "flickering" has two components: reaction which causes the patches to grow or shrink and interconvert; diffusion which causes the patches to move around in and out of the window. The former drives the transitions discussed in Fig. 2, but the latter can dominate behavior when time series come from a subwindow and can also potentially produce transitions on a much shorter time scale.

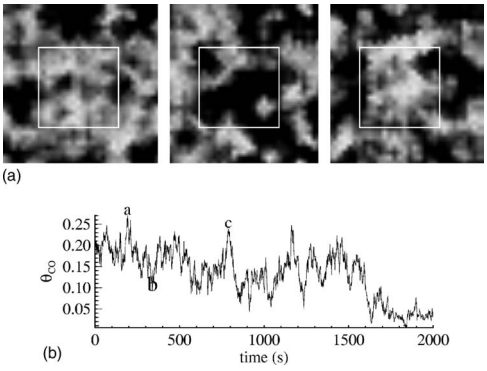

FIG. 5. Top: snapshots from a hysteresis simulation of CO oxidation in a 32×32 site system at three different times labeled by *a*, *b*, and *c* in the bottom frame. Lighter color means higher CO coverage. Bottom: CO coverage for the 16×16 site subsystem indicated by a white square.

It should be emphasized that this picture relies on the coexistence of nanometer-sized patches of different types separated by atomically sharp boundaries or interfaces. Most studies of reaction-diffusion systems have considered the mean-field regime of higher T or lower P where boundaries between coexisting states are diffuse (on the scale of microns). The occurrence of sharp boundaries in our studies reflects the different conditions where interactions are strong and phase separation can occur.

In summary, fluctuation behavior and pattern formation is shown to be more complex in nanoscale reaction systems at higher P than in previous mean-field reaction modeling. However, with application of a realistic atomistic model, we can capture behavior which derives from reactant phase separation.

This work was supported by the Division of Chemical Sciences, USDOE-BES. It was performed at Ames Laboratory, operated for the USDOE by ISU under Contract No. W-7405-Eng-82.

[1] V. Johánek, M. Laurin, A. W. Grant, B. Kasemo, C. R. Henry, and J. Libuda, Science **304**, 1639 (2004).
[2] Y. Suchorski, J. Beben, E. W. James, J. W. Evans, and R. Imbihl, Phys. Rev. Lett. **82**, 1907 (1999).
[3] R. Imbihl and G. Ertl, Chem. Rev. (Washington, D.C.) **95**, 697 (1995).
[4] J. W. Evans, D.-J. Liu, and M. Tammaro, Chaos **12**, 131 (2002).
[5] D.-J. Liu, N. Pavlenko, and J. W. Evans, J. Stat. Phys. **114**, 101 (2004).
[6] D.-J. Liu and J. W. Evans, J. Chem. Phys. **117**, 7319 (2002).
[7] V. P. Zhdanov and B. Kasemo, Surf. Sci. Rep. **39**, 25 (2000).
[8] M. Pineda, R. Imbihl, L. Schimansky-Geir, and C. Zülicke, J. Chem. Phys. **124**, 044701 (2006).
[9] M. F. H. van Tol, A. Gielbert, and B. E. Nieuwenhuys, Catal. Lett. **16**, 297 (1992).
[10] V. Gorodetskii, J. H. Block, W. Drachsel, and M. Ehsasi, Appl. Surf. Sci. **67**, 198 (1993).
[11] V. V. Gorodetskii, V. I. Elokhin, J. W. Bakker, and B. E. Nieuwenhuys, Catal. Today **105**, 183 (2005).
[12] J. Libuda and H.-J. Freund, Surf. Sci. Rep. **57**, 157 (2005).
[13] D.-J. Liu and J. W. Evans, J. Chem. Phys. **124**, 154705 (2006).
[14] R. M. Ziff and B. J. Brosilow, Phys. Rev. A **46**, 4630 (1992).